Clinical Neurology and Neurosurgery 167 (2018) 43–53

Contents lists available at ScienceDirect

Clinical Neurology and Neurosurgery

journal homepage: www.elsevier.com/locate/clineuro

Genotype, phenotype and *in silico* pathogenicity analysis of *HEXB* mutations: Panel based sequencing for differential diagnosis of gangliosidosis

Nejat Mahdieh[a], Sahar Mikaeeli[a], Ali Reza Tavasoli[b,c], Zahra Rezaei[b], Majid Maleki[a], Bahareh Rabbani[a,c,*]

[a] Genetic Research Center, Rajaie Cardiovascular Medical and Research Center, Iran University of Medical Sciences, Tehran, Iran
[b] Children's Hospital Center, Pediatric Center of Excellence, Tehran University of Medical Center, Tehran, Iran
[c] Growth and Development Research, Tehran University of Medical Sciences, Tehran, Iran

ARTICLE INFO

Keywords:
HEX B variants
Gangliosidosis
Next generation sequencing
In silico analysis

ABSTRACT

Objectives: Gangliosidosis is an inherited metabolic disorder causing neurodegeneration and motor regression. Preventive diagnosis is the first choice for the affected families due to lack of straightforward therapy. Genetic studies could confirm the diagnosis and help families for carrier screening and prenatal diagnosis. An update of *HEXB* gene variants concerning genotype, phenotype and *in silico* analysis are presented.

Patients and Methods: Panel based next generation sequencing and direct sequencing of four cases were performed to confirm the clinical diagnosis and for reproductive planning. Bioinformatic analyses of the *HEXB* mutation database were also performed.

Results: Direct sequencing of *HEXA* and *HEXB* genes showed recurrent homozygous variants at c.509G > A (p.Arg170Gln) and c.850C > T (p.Arg284Ter), respectively. A novel variant at c.416T > A (p.Leu139Gln) was identified in the *GLB1* gene. Panel based next generation sequencing was performed for an undiagnosed patient which showed a novel mutation at c.1602C > A (p.Cys534Ter) of *HEXB* gene. Bioinformatic analysis of the *HEXB* mutation database showed 97% consistency of *in silico* genotype analysis with the phenotype. Bioinformatic analysis of the novel variants predicted to be disease causing. *In silico* structural and functional analysis of the novel variants showed structural effect of *HEXB* and functional effect of *GLB1* variants which would provide fast analysis of novel variants.

Conclusions: Panel based studies could be performed for overlapping symptomatic patients. Consequently, genetic testing would help affected families for patients' management, carrier detection, and family planning's.

1. Introduction

Gangliosides are main components of the neuronal plasma membrane. Six major gangliosides have been identified; GM1 and GM2 gangliosidoses are major fatal neurodegenerative diseases due to defects in ganglioside catabolism. The clinical manifestation of gangliosidosis correlates with the different substrates that are stored and not catabolized e.g GM1 and GM2 gangliosidoses; GM1-gangliosidosis has deficiency of B-galactosidase (*GLB1* gene, MIM 611458) [1]. *GLB1* gene is located at 3p22.3 and contains 16 exons. β-galactosidase breaks downs several molecules including GM1 gangliosidase, oligosaccharides and keratan sulfate.GM2 ganglioside is the substrate for B-hexaminidase A which is deficient in GM2-gangliosidosis including Tay-Sachs, Sandhoff (MIM 268800), and variant AB.

The deficiency of hexosaminidase A and B [Hex A (heterodimer α and β subunits) and Hex B (homodimer of β subunits)] activity is seen in Sandhoff disease, but only Hex A deficiency is seen in Tay-Sachs disease. Sandhoff disease inherited with autosomal recessive inheritance is caused by defect in lysosomal B-hexosaminidase A, composed of α chain, β chain and GM2-activator proteins [2,3]. Symptoms of these two disorders may overlap with GM1 gangliosidosis which can make the diagnosis difficult. There are different phenotypes for gangliosidosis based on biochemical findings and age of onset; infantile (acute form; < 0.1% activity), late infantile and juvenile (subacute form; 0.5% activity) and adult (chronic; 2–4% activity) forms [4]. Mutations in the individual proteins of the B-hexosaminidase enzyme complex cause different levels of activity and structural changes.

Sandhoff disease is caused by mutations in *HEXB* gene, which encodes the beta chain, located on 5q13 chromosome, encompassing 14 exons, spanning 2 Kb mRNA and encoding 556 amino acids. *HEXA* encodes the α chain, located on 15q23-q24, which mutations clinically cause Tay-Sachs disease [2,5]. These two genes have approximately

* Corresponding author at: Genetic Research Center, Rajaie Cardiovascular Medical and Research Center, Iran University of Medical Sciences, P.O. Box: 1996911151, Tehran, Iran.
E-mail addresses: nmahdieh@rhc.ac.ir (N. Mahdieh), baharehrabbani@yahoo.com (B. Rabbani).

https://doi.org/10.1016/j.clineuro.2018.02.011
Received 25 July 2017; Received in revised form 31 January 2018; Accepted 5 February 2018
Available online 08 February 2018
0303-8467/

60% similarity in function and structure [5,6,7]. In addition, *GM2A* gene, the other component of hexoaminidase A complex, acts as substrate specific co-factor causing AB-variant phenotype. Mutations in any of the three related gene products of B-hexsoaminidase A protein lead to GM2 accumulation in neuronal lysosomes and cause fatal neurodegeneration and apoptosis of neurons [8].

To date, 182 mutations for *HEXA*, 105 for *HEXB* gene and 9 for *GM2A* have been reported in the Human Gene Mutation Database (HGMD) to cause GM2 gangliosidosis (www.hgmd.org). Also, 211 mutations have been reported for *GLB1* gene in HGMD.

We report a case suspected of having gangliosidosis with unspecific biochemical and enzymatic findings, and patients clinically diagnosed with Sandhoff disease, Tay-Sachs disease, and GM1-gangliosidosis. Molecular genetic diagnosis was established by panel based next generation sequencing for the suspected case and by direct sequencing for clinically diagnosed patients. *In silico* structural and functional analyses were performed to evaluate novel variants and to predict pathogenicity. In addition, we provide a literature review of the spectrum of *HEXB* gene mutations described in Sandhoff disease performed up to December 2017.

2. Patients and methods

2.1. Genetic testing

We studied four patients from Iranian population. Informed consent was obtained and DNA for genetic testing was extracted from peripheral blood using standard protocols. Coding regions and exon-intron boundaries were enriched using NimleGen kit (NimbleGen, Roche, Basel, Switzerland). Sequencing analysis was performed for first case by targeted-next generation sequencing (NGS) on an Illumina, Hiseq2000 (Illumina, San Diego, California, USA). Reads were aligned using Burrows–Wheeler Aligner (BWA) on reference genome (hg19) [9]. Variants should have been annotated; annotation was performed by SAMTools [10]. Gangliosidosis genes [11] including 4 genes (*HEXB, HEXA, GM2A* and *GLB1*) were used as a pane for analysis. For finding rare variants, they were filtered based on their frequency (minor allele frequency < 0.01) in 1000 Genome and dbSNP [12] (https://www.ncbi.nlm.nih.gov/projects/SNP/). Variants were validated based on sequencing analysis and segregation analysis of the patients. Coverage of target region with at least depth of 30X was approximately 99%.

Direct sequencing of *HEXB, HEXA* gene and *GLB1* gene was performed for clinically diagnosed patients (#2-4).

2.2. Case presentation

2.2.1. Case 1

A 10 month old boy referred to Children's Hospital Center with nystagmus, weakness and wasting of limb muscles. He was born after a full term pregnancy with head circumference of 35 cM and birth weight of 3.450 Kg from a first cousin couple. His older brother had no related clinical symptoms. No other affected family member was seen.

The clinical onset of symptoms began at 5 months of age with nystagmus and hypotonia but parents did not seek pediatrician consultation until 10 months old. He had developmental delay since the early months of life and regressed in later months. Speech was initially delayed, then became absent as he aged. In addition regression of motor skills and cognition was noticed.

Physical examination revealed head circumference of 46 cM, dysmorphic features, hypoacusis, startle reaction to loud noise and no organomegaly. He had uprolling of eyes and tonic contraction of limbs. Sonography of the abdomen was also normal. Neurological examination showed hypotonia of limbs. Ophtlamolgical examination showed presence of bilateral cherry-red spots. Auditory brainstem response (ABR) was normal. Cerebral computed tomography (CT) scanning showed a bilateral thalamic hyperdensity with hypodensity of the white matter. Magnetic resonance imaging (MRI) revealed increased signal intensity on T1-weighted images in thalamus and hypointense on T2-weighted images.

Enzyme analysis showed deficiency of hexosaminidase B-HexA and HexB in serum. Beta galactosidase activity was lower (< 0.017) than normal range (0.017–0.048 unit nmol/mg). Serum alanine aminotransferase (ALT or glutamic pyruvic transaminase = SGPT) was 126 (normal level: 7-57 U/L) and aspartate aminotransferase (AST or glutamic oxaloacetic transaminase = SGOT) level was 146 (normal range: 5-40U/L). Clinical data suggested gangliosidosis.

2.2.2. Case 2

A couple referred for prenatal diagnosis having a child clinically diagnosed with Sandhoff disease. Their child was a 21 month old boy having nystagmus, muscle weakness, problems in walking and delayed motor skills. He was the first child of this healthy consanguineous couple, although they had similar disease in the mother's cousin. The onset of the disease began at 6 months. He had cognitive, speech and motor delay and regression. On physical examination hepatosplenmegaly, hypotonia and limb spasticity were noted. He lost the ability to perform tasks and decreased eye movements. Ophthalmologic examination showed bilateral cherry red spots. HPLC biochemical analysis of amino acids was normal. Tandem mass spectrometry (MS/MS) showed no significant deficiency of fatty acids and amino acids. Liver function tests (LFT) were normal. Enzyme assay of the activity of hexaminidase A and Hex B revealed deficiency; consequently, the clinical diagnosis of Sandhoff disease was made at the age one year old.

2.2.3. Case 3

A one year old girl with neurologic regression in the first year of life referred to genetic laboratory for molecular testing of *GLB1* gene. She was the first child of healthy consanguineous parents. She had developmental delay beginning at 3 months old. She also had hearing problems. She presented hypotonia and hepatosplenomegaly. β-galactosidase activity was very low.

2.2.4. Case 4

A one year and 9 months old girl referred to Children's Hospital Center. She was born as the first child of consanguineous parents. She had normal growth and development until 6 months of age. Motor regression appeared by this age. Ophthalmology examination showed right sided strabismus. She was also diagnosed with Chronic Rhinosinusitis. Mucopolysaccharide urine analysis of MPSI, MPSII, MPSVI and GM1 analysis were in normal range. Tandem mass spectrometry (MS/MS) analysis of the specific metabolic enzymes was normal. She developed hyperaucosis but no organomegaly was noted, therefore, she was clinically suspected to have GM2 gangliosidosis. Enzyme assay reveled deficiency of Hex A while Hex AB and Hex B were normal. She was clinically diagnosed with Tay-Sachs disease.

2.3. In silico structural and functional analyses of HEXB and GLB1 novel variants

Position of each identified variant was determined based on *HEXB* gene reference sequence: NP_000512.1 and NM_000521.3. *In silico* analysis was performed for all the reported variants to determine pathogenicity of the variants by MutationTaster [13], SIFT [14], and PROVEAN (Protein Variation Effect Analyzer) [15]. CADD (Combined Annotation Dependent Depletion) was software used to characterize the pathogenicity of variants in the studied cases [16].

Structural analysis was based on Phyre2 and I-TASSER servers. Structural analysis was based on protein homology/analogy recognition engine V2.0 (Phyre2) [17] to determine the structure and function of the variants in protein [18]. Iterative threading assembly refinement (I-TASSER) server was also applied for protein structure and function predictions [19]. The protein sequence of hexaminidase B and B-

galactosidase was aligned using UniProtKB/Swiss-Prot P07686 and P16278.2, respectively.

2.4. Interactome analysis

Interaction of the protein in relation to other proteins was investigated by STRING10 to describe the cause of phenotypic variability and/or overlapping phenotypes [20].

2.5. Literature review

A literature review of *HEXB* gene mutations in PubMed was performed using keywords "*HEXB* gene, "mutation", "gene" and "Sandhoff disease"; in addition, HGMD and *HEXB* database (Hexdb.mcgill.ca) were searched to identify all the published mutations up to December 2017. The typical and atypical cases within the populations and related phenotype were identified within *HEXB* database. The population of the variants of HEXB gene was also determined wherever possible. All mutations were named based on human genome variation database (HGVS). Duplicated variants and results were excluded.

3. Results

3.1. Molecular characterization of cases

3.1.1. Case 1

NGS panel for the case showed a homozygous mutation at position c.1602C > A of *HEXB* gene in exon 13 leading to a premature stop codon (Cys534Ter). As a consequence segregation analysis confirmed the result.

3.1.2. Case 2

Sanger sequencing of *HEXB* gene revealed a homozygous mutation at c.850C > T encoding p.Arg284Ter (rs121907986) which leads to a stop codon. Segregation analysis confirmed heterozygous mutation in the parents. Prenatal diagnosis was performed for a subsequent pregnancy.

3.1.3. Case 3

Molecular analysis and Sanger sequencing of GM1-gangliosidosis showed a homozygous variant at c.416T > A (p.Leu139Gln) on *GLB1*gene. Segregation analysis also confirmed heterozygous mutation for the parents.

3.1.4. Case 4

Direct sequencing of *HEXA* gene showed a homozygous mutation at c.509G > A causing a missense change p.Arg170Gln (rs121907957) in exon 5 *HEXA* gene.

3.2. Mutation and data selection

Data from HGMD database (Professional 2016) showed 105 mutations for *HEXB* gene. Our search in published data, papers and ClinVar database revealed 107 mutations. The pathogenic variants were categorized based on the position of gene, amino acid change, rs#, clinical phenotype, origin, and functional effect of mutations (Table 1). *In silico* analysis was performed for each variant to compare the results with *in vivo* phenotypes (Table 1).

The collected *HEXB* mutations (Table 1) showed that the mutations occurred in *HEXB* gene were mainly missense accounting for 39.25% of mutations; other types of mutation included 26.16% deletion, 19.62% splicing, 10.28% nonsense, and 4.67% insertion in the gene (Table 1). In total, 30.84% of mutations were predicted to lead to truncated proteins caused by ins/dels and 10.28% lead to stop codons. 75.7% of the mutations were exonic and 24.39% were non-coding mutations. Most of the mutations clustered in exon 13 (15.88%), and in exon 1, exon 7 and 11 (each included about 10% of mutations) (Fig. 1).

3.3. Phenotype analysis

26 variants showed infantile Sandhoff disease, 7 juvenile form, 9 late/adult form and 56 described variants did not indicate the time of onset. Five mutations were clinically seen both in IS and JS. One mutation in *HEX B* was clinically diagnosed as Tay-Sachs disease. Also, two mutations showed chronic adult onset Sandhoff disease (Table 1). Approximately, 70% of the mutations had known ethnicity and the remaining were not differentiated for the ethnic group of the cases.

3.4. Variant position and influence in the predicted secondary structure

The amino acid sequence and the secondary structure, and domains of Hex B were determined *in silico* and the reported variants were shown (Fig. 2). The position of reported variants was depicted to evaluate the effect of variants on secondary structure, domains and segments. Most variants (23.36%) were gathered in predicated docking site which contributes in interaction of the GM2 activator protein with the GM2 gangliosides for degradation of gangliosides.

3.5. Pathogenicity

Variant annotation was performed using online tools. MutationTaster predicted a disease causing mutation at position c.1602C > A (p.Cys534Ter) of *HEXB* gene for the first case; the software predicted that the helix formed by amino acid 522–538 was lost; in addition a disulfide bond at position 534, and 551 were lost. 546–548 forming the strand was also lost. Less than 10% of protein length was predicted to be lost and cause non-sense mediated decay (NMD). PhastCons was 1 (range: not conserved 0–1 conserved) which shows the conservation of the sequence. PhyloP value was 1.466 (range: −14 to +6) which shows the conservation without neighboring effect-positive value show slower evolutionary changes while negative values show faster changes. As this nucleotide substitution will lead to stop codon it causes termination which is expected to cause the disorder. CADD analysis showed high PHRED score of 24.2 which is predicted to be highly deleterious and is categorized under pathogenic variants.

In silico analysis of variant in Case 3, c.416T > A (p.Leu139Gln) in *GLB1* was predicted to be disease causing by MutationTaster, damaging by SIFT and probably damaging by PolyPhen. PhyloP value was 3.482 and PhastCons was 1 (0–1; conserved). It is predicted that the helix protein feature is affected. CADD analysis showed PHRED score 28.4, predicted to be pathogenic.

102 variants out of which 97 (95%) were predicted to be disease causing by MutationTaster and confirmed the phenotypes. Five reported variants predicted to be polymorphism but the clinically diagnosed with Sandhoff disease. 88% of substitution variants were predicted to affect protein function by SIFT. PROVEAN analysis was performed for substitutions and small indels (65 positions) with consistency of 90% (45/50) of the variants to the phenotype. Therefore, it could be concluded that *in silico* analysis could be performed for fast analysis of pathogenicity of reported mutations; although we might miss some of the pathogenic effect.

3.6. In silico structural and functional analyses of novel variants

Structure analysis of p.Cys534Ter in Hex B by Phyre2 was modeled based on c1nouA (native human lysosomal beta-hexosaminidase isoform b) with 99% identity and 100% confidence. As shown, the alpha helix structure at amino acid 534 is predicted to be disordered with high score and the secondary structure was predicted to change (Table 2). This means that low disordered regions are lower in flexibility, dynamicity and lower extension in solution and sensitive to a

Table 1
Reported mutations of *HEXB* gene in databases.

No.	Mutation		Region	Origin	Rs#	Consequence					References
	DNA level	Amino acid level				DNA level	Phenotype	*In silico*			
								MutationTaster	Provean	SIFT	
	Deletions										
1	c.115delG	p.Val39TrpfsX25	Exon1	Canada	rs398123443	Frameshift	IS	DC	Neutral	NA	[21]
2	c.171delG	p.Trp57CysfsX7	Exon1	Spain	rs771973471	Frameshift	IS	DC	Deleterious	NA	[22]
3	c.176delT	p.Leu59ArgfsX5	Exon1	France	_	Frameshift	JS	DC	Deleterious	NA	[23]
4	c.550delT	p.Tyr184MetfsX23	Exon4	Iran	_	Frameshift	IS	DC	NA	NA	[24]
5	c.800-817del	p.Thr267_Arg272del	Exon7	Spain	_	Deletion	IS/JS	DC	NA	NA	[22]
6	c.1021delA	p.Ser341ValfsX30	Exon8	_	–	Frameshift	AS	DC	Deleterious	NA	[25][26][39]
7	c.1057-159delGGA	p.Gly353del	Exon8	_	rs1665894	Deletion	IS/JS	DC	NA	NA	[26]
8	c.1238_1242delCAAAG	p.Lys414CysfsX7	Exon10	_	rs398123445	Frameshift	S	DC	–	–	clinvar
9	c.1260-1265delAGTTGA	p.Val421-Glu422del	Exon11	China	_	Frameshift	S	DC	–	–	[27]
10	c.1404delT	p.Pro468ProfsX62	Exon11	China	_	Frameshift	JS	DC	Deleterious	NA	[28]
11	c.1535_1536delGA	p.Arg512ThrfsX12	Exon13	_	rs794727091	Frameshift	S	DC	NA	NA	clinvar
12	c.1552delG	p.Asp518MetfsX12	Exon13	Iran	_	Frameshift	IS	DC	NA	NA	[24]
13	c.76delA	p.Met26CysfsX5	Exon1	Cyprus	_	Frameshift	S	DC	Neutral	NA	[29]
14	c.534delAGTT	p.Leu178PhefsX28	Exon4	Italy	_	Frameshift	IS	DC	NA	NA	[30]
15	c.772delG	p.Gly258GlufsX17	Exon7	_	_	Frameshift	IS	DC	NA	NA	[31]
16	c.782delCTTT	p.Ser261CysfsX13	Exon7	Argentina	_	Frameshift	S	DC	NA	NA	[32]
17	c.825delT	p.Ile275MetfsX32	Exon7	_		Frameshift	S	DC	NA	NA	[33]
18	c.965delT	p.Ile322fsX32	Exon8	Italy	rs768438206	Frameshift	S	DC	Deleterious	NA	[34]
19	c.1169 + 3_1169 + 10delAAGTTGTT	p.Glu362ValfsX168	Exon9	Saudi Arabia	rs398123444	Frameshift	S	DC	–	–	[35]
20	c.1303delAG	p.Arg435SerfsX20	Exon11	_	rs779328596	Frameshift	IS	DC	NA	NA	[31]
21	c.1345delT	p.Trp449GlyfsX3	Exon11	_	_	Frameshift	IS	DC	Deleterious	NA	[36]
22	c.534_541delAGTTTATC	p.Val179ArgfsX10	Exon4	India	_	Frameshift	S	DC	NA	NA	[37]
23	c.1563_1573delTATGGATGACG	p.Met522LeufsX2	Exon13	India		Frameshift	S	DC	NA	NA	[37]
24	c.299 + 1471_408del2406	–	Gross deletion (IVS1)	Italy	_	–	S	–	–	–	[34]
25	15089bpdel	–	Gross deletion (LCR)	_	–	–	S	–	–	–	[38]
26	Del16kb	–	Gross deletion (3'UTR)	South Korea	–	–	IS	–	–	–	[39,40]
27	Del16kb	–	Gross deletion (5' end to IVS5)	_	–	–	S	–	–	–	[41]
28	Del50kb	–	Gross deletion (5'-promoter-IVS6)	_	_	–	IS	_	–	–	[42]
	Duplication/insertion										
29	c.1484-1486dupCAA	p.Thr496dup	Exon12	_	rs1665894	Insertion	IS/JS	DC	NA	NA	[26]
30	c.1517_1529dupCAAGTGCTGTTGG	p.Glu511LysfsX5	Exon13	_	rs797044644	Frameshift	S	DC	NA	NA	clinvar
31	c.1553_1554insAAGA	p.Asp518GlufsX8	Exon13	India	_	Frameshift	S	DC	–	–	[37]
32	c.1591_1592insC	p.Arg531ThrfsX22	Exon13	India		Frameshift	S	DC	NA	NA	[37]
33	18IVS13insTTCATGTTATCTACAGAC	_	IVS13/exon14	_	–	In frame Insertion	JS	–	–	–	[43]
	Substitution										
34	c.171G > C	p.Trp57Cys	Exon1	France		Missense	IS	DC	Deleterious	APF	[23]
35	c.289G > C	p.Ala97Pro	Exon1	_	_	Missense		DC	Deleterious	APF	[26]
36	c.299G > T	p.Arg100Leu	Exon1	Italy	_	Missense	S	DC	Deleterious	APF	[34]
37	c.362A > G	p.Lys121Arg	Exon2	Japan	rs11556045	Missense	IS	polymorphism	Neutral	Tolerate	[44]
38	c.410G > A	p.Cys137Tyr	Exon2	_	rs779453450	Missense	IS	DC	Deleterious	APF	[45]
39	c.448A > C	p.Thr150Pro	Exon3	Italy	_	Missense	S	polymorphism	Neutral	Tolerate	[27]
40	c.611G > A	p.Gly204Glu	Exon5	India	rs762821794	Missense	S	DC	Deleterious	APF	[37]
41	c.619A > G	p.Ile207Val	Exon5	Canada	rs10805890	Missense	AS + motor nervous disease	polymorphism	Neutral	Tolerated	[46]
42	c.626C > T	p.Thr209Ile	Exon5	Italy	_	Missense	S	DC	Deleterious	APF	[27]

(*continued on next page*)

Table 1 (*continued*)

No.	Mutation		Region	Origin	Rs#	Consequence					References
	DNA level	Amino acid level				DNA level	Phenotype	*In silico*			
								MutationTaster	Provean	SIFT	
43	c.634C > A	p.His212Asn	Exon6	Brazil	_	Missense	S	DC	Deleterious	APF	[27]
44	c. 634A > T	p.His212Tyr	Exon6	India	_	Missense	S	DC	Deleterious	APF	[37]
45	c.668T > C	p.Leu223Pro	Exon6	China	rs367963796	Missense	S	DC	Deleterious	APF	[47][22]
46	c.703C > T	p.His235Tyr	Exon6	_	_	Missense	AS	DC	Deleterious	APF	[48]
47	c.765C > G	p.Ser255Arg	Exon 6	Japan		Missense	IS	DC	Deleterious	Tolerated	[44]
48	c.793G > T	p.Val265Phe	Exon7	France	_	Missense	IS	DC	Deleterious	APF	[23]
49	c.796T > G	p.Tyr266Asp	Exon7	Spain	rs373979283	Missense		DC	Deleterious	APF	[22]
50	c.845G > A	p.Gly282Glu	Exon7	Spain	_	Missense		DC	Deleterious	APF	[22]
51	c.851G > A	p.Arg284Gln	Exon7	Turkey	_	Missense	JS	DC	Deleterious	APF	[49][58]
52	c.884C > G	p.Thr295Arg	Exon7	_	_	Missense		DC	Deleterious	APF	[26]
53	c.926G > A	p.Cys309Tyr	Exon8	Italy		Missense	AS	DC	Deleterious	APF	[50]
54	c.926G > T	p.Cys309Phe	Exon8	Italy	_	Missense	S	DC	Deleterious	APF	[27]
55	c.1078T > C	p.Cys360Arg	Exon8	_	_	Missense		DC	Deleterious	APF	[26]
56	c.1250C > T	p.Pro417Leu	Exon11	Italy	rs28942073	Missense	AS	DC	Deleterious	APF	[50]
57	c.1309A > C	p.Thr437Pro	Exon11	Korea	_	Missense	IS	DC	Deleterious	APF	[39]
58	c.1367A > C	p.Tyr456Ser	Exon11	Canada	rs121907982	Missense	AS + motor nervous disease	DC	Deleterious	APF	[46]
59	c.1376A > C	p.Asp459Ala	Exon11	_	_	Missense	JS	DC	Deleterious	APF	[51]
60	c.1447G > A	p.Gly483Ser	Exon12	_	_	Missense	IS	DC	Deleterious	APF	[52][61]
61	c.1451G > A	p.Gly484Glu	Exon12	Argentina	_	Missense	S	DC	Deleterious	APF	[27]
62	c.1481A > G	p.Asp494Gly	Exon12	_	_	Missense	S	DC	Deleterious	APF	[53]
63	c.1507T > C	p.Trp503Arg	Exon13	_	_	Missense		DC	Deleterious	APF	[26]
64	c.1510C > T	p.Pro504Ser	Exon13	French Canadian	rs121907985	Missense	CS	DC	Deleterious	APF	[54]
65	c.1514G > A	p.Arg505Gln	Exon13	_	rs121907983	Missense	AS	DC	Deleterious	APF	[55]
66	c.1538T > C	p.Leu513Pro	Exon13	_	rs778501777	Missense		DC	Deleterious	APF	[26]
67	c.1598A > G	p.Asp494Gly	Exon13	_		Missense	CS	DC	Deleterious	APF	[53]
68	c.1597C > T	p.Arg533Cys	Exon13	Saudi Arabia	rs764552042	Missense	S	DC	Deleterious	APF	[35]
69	c.1598G > A	p.Arg533His	Exon13	Japan	_	Missense	AS	DC	Deleterious	APF	[56]
70	c.1601G > A	p.Cys534Tyr	Exon13	Japan	_	Missense	IS	DC	Deleterious	APF	[57]
71	c.1601G > T	p.Cys534phe	Exon13	Canada	rs727503960	Missense	S	DC	Deleterious	APF	[58]
72	c.1615C > T	p.Arg539Cys	Exon14	Spain	rs749646826	Missense		DC	Deleterious	APF	[22]
73	c.1627G > A	p.Ala543Thr	Exon14	Jews and Arabs	rs121907984	Missense	TSD	DC	Deleterious	Tolerate	[59]
74	c.1645G > A	p.Gly549Arg	Exon14	China	rs398123448	Missense	IS	DC	Deleterious	APF	[60]
75	c.1652G > A	p.Cys551Tyr	Exon14	Canada	rs727503961	Missense	S	DC	Deleterious	APF	[58]
76	c.94C > T	p.Gln32X	Exon1	Saudi Arabia	_	Nonsense	S	DC	–	–	[35]
77	c.146C > A	p.Ser49X	Exon1	Bulgaria	_	Nonsense	S	DC	–	–	[27]
78	c.298C > T	p.Arg100X	Exon1	India	_	Nonsense	S	DC	–	–	[37]
79	c.333G > A	p.Trp111X	Exon2	India	rs761117459	Nonsense	S	DC	–	–	[37]
80	c.508C > T	p.Arg170X	Exon3	Spain	rs753823903	Nonsense		DC	–	–	[22]
81	c.552T > G	p.Tyr184X	Exon4	_	rs573447174	Nonsense	IS/JS	DC	–	–	[26]
82	c.850C > T	p.Arg284X	Exon7	_	rs121907986	Nonsense	IS	DC	–	–	[36]
83	c.1372C > T	p.Gln458X	Exon11	Italy	_	Nonsense	S	DC	–	–	[34]
84	c.1389C > G	p.Tyr463X	Exon11	China	_	Nonsense	S	DC	–	–	[47][22]
85	c.1541G > A	p.Trp514X	Exon13	Spain		Nonsense		DC	–	–	[22]
86	c.1602C > A	p.Cys534X	Exon13	Iran	_	Nonsense	S	DC	–	–	This study
	Splicing										
87	c.299 + 5G > A	–	IVS1	_	_	–	IS	DC	–	–	[61][69]
88	c.299 − 2A > G	–	IVS1	Italy	_	–	IS	DC	–	–	[34]
89	c.299 − 1G > T	–	IVS1	Italy	_	–	S	DC	–	–	[34]
90	c.445 + 1G > A	–	IVS2	Argentina	_	–	S	DC	–	–	[62]

(*continued on next page*)

Table 1 (*continued*)

No.	Mutation		Region	Origin	Rs#	Consequence					References
	DNA level	Amino acid level				DNA level	Phenotype	*In silico*			
								MutationTaster	Provean	SIFT	
91	c.445 − 1G > A	–	IVS2	Japan	–	–	AS	DC	–	–	[56]
92	c.511 − 1G > T	–	IVS3	Italy	–	–	S	DC	–	–	[34]
93	c.558 + 5G > A	–	IVS4	France	–	Splicing…	IS/JS	DC	–	–	[23]
94	c.901 − 2A > G		IVS7		rs756337388			DC	–	–	[26]
95	c.901 − 48T	–	IVS7	China	–	–	IS		–	–	[60]
96	c.1082 + 5G > C	–	IVS8	Greek-Cypriot	rs5030731	–	S	DC	–	–	[63]
97	c.1082 + 5G > A	–	IVS8	Argentina	rs5030731	–	S	DC	–	–	[27]
98	c.1082 + 5 G > T		IVS8	India	–		S	DC	–	–	[37]
99	c.1169 + 5G > A	–	IVS9	Brazil	–	–	S	DC	–	–	[27]
100	c.1242 − 1G > A	–	IVS10	–	–	–	IS	DC	–	–	[64]
101	c.1242 − 3T > G		IVS10	–	–			DC	–	–	[26]
102	c.1242 − 17A > G	–	IVS10	Japan	–	–	IS	polymorphism	–	–	[44]
103	c.1242 + 1G > A	–	IVS10	Argentina	rs543503758	–	S	DC	–	–	[27]
104	c.1242 + 8C > T	–	IVS10	Japan	–	–	JS	DC	–	–	[65]
105	c.1417 + 1 G > A	–	IVS11	India	–	–	S	DC	–	–	[37]
106	1508 − 26G > A	–	IVS12	–	rs201580118	–	JS	polymorphism	–	–	[66]
107	1613 + 2T > G	–	IVS13	–	rs750658080	–	IS	DC	–	–	[67]

S: Sandhoff disease; IS: Infantile Sandhoff; JS: Juvenile Sandhoff; AS: Adult Sandhoff; CS: chronic Sandhoff; Tay-Sachs disease (TSD); ND: not determined; DC: disease causing; D: Deleterious; APF: Affect protein function.

change. Normal sequence was predicted to be helix by I-TASSER but it is predicted to be coil within the cystein 534 changing to stop codon. The predicted solvent accessibility at this position was changed from score 4 (normal) to score 5 (mutant) (ranges: 0 = buried to 9 = exposed). This shows that the protein at this position is more exposed than normal sequence. The BFP value was 1.47 for C534 predicting to be unstable, instead the BFP for normal sequence at this position was −0.47 showing helix and being exposed comparing to becoming coiled and buried (Table 2).

The ligand binding sites were predicted based on different PDB models by I-TASSER in truncated protein compared to the normal protein. The amino acids binding positions –*e.g.* 211,294,354,355,405,424,450,452,489,491- were the sites of binding with different ligands. Enzyme function was slightly changed based on PDB 1o7aA from C-score^{EC} 0.651 to 0.617; in addition the active site at 354, 355 was not affected in the truncated protein based on PDB1o7aA. The C-score^{GO} based on gene ontology was changed from 0.62 to 0.51 (Data not shown). Phyre2 functional analysis revealed predicted binding sites at Arg211, His294, Asp354, Glu355, Trp405, Trp424, Tyr450, Asp452, Leu453, Trp489, and Glu491 positions to be affected. Number of contacts was changed for these amino acids. The conservation at position 211, 345, 450, 452, 489, 491 were very high and were predicted to be more prone to the termination (Data not shown). Consequently, the termination codon is predicted to manifest changes in the function of protein and binding sites comparing to normal Hexosaminidase.

Structural analysis based on PHYRE was performed for the p.Leu139Gln in *GLB1* gene (gangliosidosis) based on c3thdD (crystal structure of human beta-galactosidase in complex with 1–2 deoxygalactonojirimycin). As shown, due to amino acid change (p.Leu139Gln) there was a slight change comparing the normal and mutated structure. I-TASSER analysis for *GLB1* was based on 3thcA (Crystal structure of human beta-galactosidase in complex with galactose). No significant change in the structure but the functional analysis by I-TASSER (COACH tool) showed slight changes (Table 2). Therefore we could conclude that the structure was affected in HEX B analysis but the function was affected in *GLB1* (galactosidase).

4. Discussion

To date, 107 different mutations have been identified in the *HEXB* gene leading to Sandhoff disease (Table1). In our case series study, targeted panel based sequencing was performed due to clinical variability and differential diagnosis of gangliosidosis. Patient 1 was deficient in HexA, HexB and B-galactosidase and showed a nonspecific phenotype which caused difficulty in clinical diagnosis. The enzyme assay for beta-galactosidase was duplicated. Leukocyte analysis was not available for assessment. Molecular analysis confirmed a homozygous mutation at *HEXB* gene (c.1602C > A mutation in exon 13). The mutation leads to elimination of the last twenty three amino acids of Hex B. Consequently, this variant as a nonsense mutation (p.Cys534Ter) is predicted to produce a truncated protein with residual activity. In Case 2, genetic testing of the proband was performed for decision making and prenatal diagnosis. The variant at position p.Arg284Ter (rs121907986) led to a stop codon. Case 3 showed variant c.416T > A (p.Leu139Gln) of the *GLB1*gene with clinical GM1 gangliosidosis. Case 4, clinically diagnosed for Tay-Sachs was confirmed for *HEXA* mutation at position c.509G > A (p.Arg170Gln). Bioinformatic tools and *in silico* structural evaluations consistent with the phenotype observed and permitted a genotype-phenotype correlation allowing for clinical prognosis of patient and provided better tools for genetic counseling within this family.

As in Case 1, *in silico* structural analysis predicted that the *HEXB* premature termination would affect the secondary structure of protein by Phyre2 and I-TASSER. The solubility and accessibility of the protein were varied. In addition, the ligand binding sites were affected; the

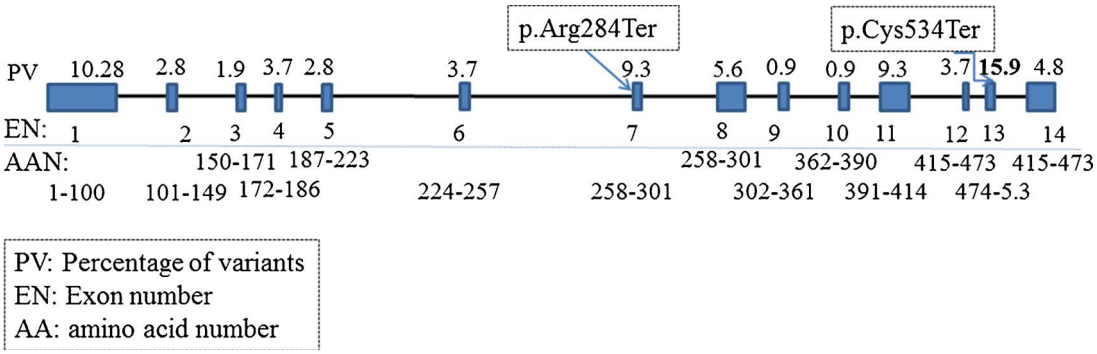

Fig. 1. Distribution and frequencies of pathogenic variants in each exon on*HEXB* gene. The variants p.Arg284Ter and p.Cys534Ter in this gene were observed in patients 1 and 2, respectively.

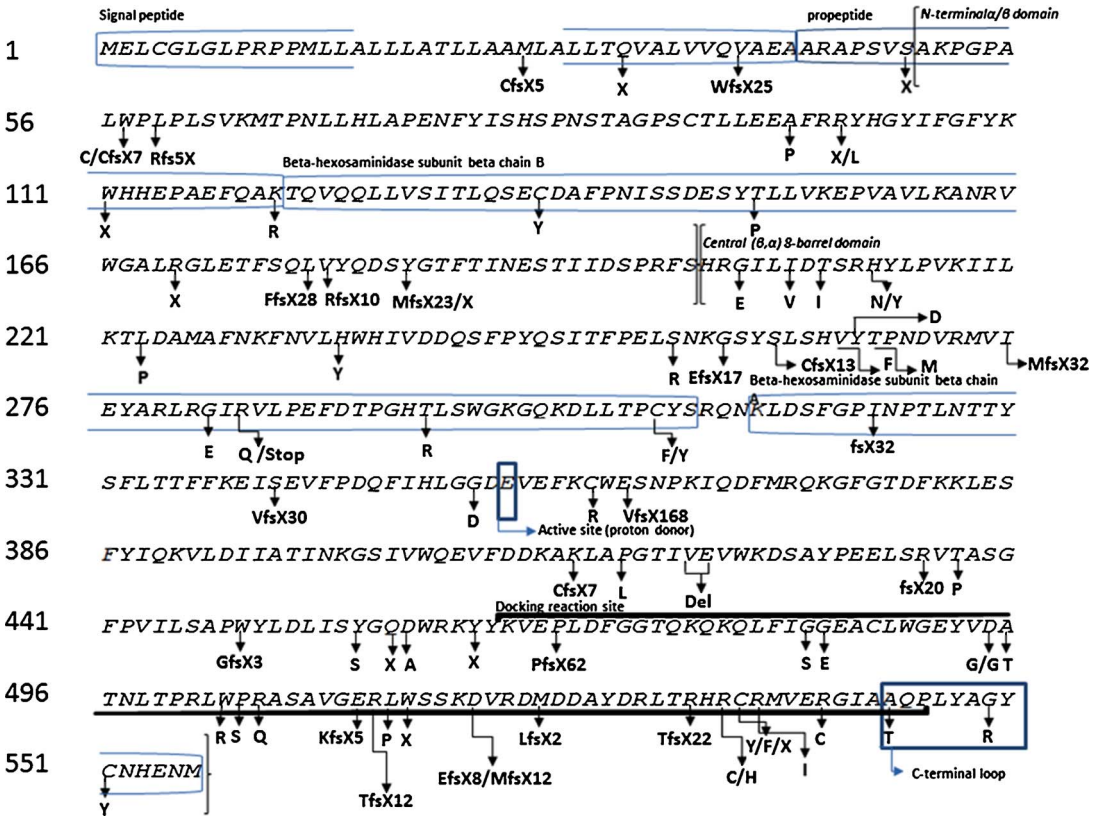

Fig. 2. The amino acid sequence of*HEX B* gene (RefSeq: NG_009770.2; RefProtein: NP_000512.1). Domains include 1–42 signal peptide, 43–121 propeptide, 122–556 chain, 122–311 forms the B chain and 315–556 forms the A chain (all marked and distinguished by names). In addition, distribution of all reported mutations in amino acid sequence of β-subunit is shown by their symbols. Furthermore, the N-terminal domain and the central (β,α) 8-barrel domain are shown between "[]" and the predicted location of docking site is shown underlined. Disulfide bonds are between 91 ↔ 137, 309 ↔ 360, 534 ↔ 551 which are not specified in this figure. The active site (a proton site at position 355), and the C-terminal loop are shown in boxes. Data extracted from http://www.uniprot.org.

function of the protein was slightly changed though the active sites were not considerably affected. This predicts that this mutation causes damage in the structure and slight change in the function. It seems that mutations in the complex would affect the structure of the protein rather than the function of the enzymes [2]. However, this may not be straightforward for hexaminidase, because early stop codons result in an unstable mRNA and abnormal protein synthesized in the ER which may be degraded [2,37]. As indicated, *in silico* structural and functional analysis (PHYRE and I-TASSER analysis) of *GLB1* gene in Case 4, predicted functional change rather than structural change due to missense (p.Leu139Gln) mutation. *GLB1* gene encodes a 677 amino acid protein (NP_000395) including 1–23 signal peptide, 24-28 propeptide, 29-677 Beta-galactosidase chain (including domain glycosyl hydrolases family 35, from 40–354, Beta-galactosidase jelly roll domain (551–619) and active sites at 188 (Proton donor) and 268 (Nucleophile) site. The defined variant at position 139 is placed at hydrolase domain. Therefore as predicted the function was more influenced rather than structure.

Existence of three B hexosaminidase isoforms (αα, αβ, ββ) indicates that each subunit has all required elements for the formation of an active site which involved in hydrolysis. The β-subunit is folded into two domains. One N-terminal α/β domain (residues 50–201) including a large six-stranded anti parallel β-sheet and a small two stranded B-sheet linked to alpha helices; the other domain includes a central $(\beta,\alpha)_8$-barrel domain (residues 202–556) including active site on C-termini of central domain (Fig. 2) [68]. 62 amino acid changes accounting for 57.94% of the mutations are seen in the central domain encoded by exon 5–14. The C-terminal contributes in dimerization (residues 543-550) accounts for the 1.76% of mutations (Fig. 1).

Table 2
: Structural and functional analysis of the p.Cys534Ter in*HEXB* and p.Leu139Gln in *GLB1* by PHYRE2 and I-TASSER tools.

	Phyre HEXB	Phyre p.Cys534Ter in *HEXB*	I-TASSER HEXB	I-TASSER p.Cys534Ter HEXB	Phyre GLB1	Phyre p.Leu139Gln in *GLB1*	I-TASSER *GLB1*	I-TASSER p.Leu139Gln in *GLB1*
Modeled based PDB Title /threading template	c1nouA native human lysosomal beta-hexosaminidase isoform b	c1nouA native human lysosomal beta-hexosaminidase isoform b	1o7aA Human beta-Hexosaminidase B	1o7aA Human beta-Hexosaminidase B	c3thdD crystal structure of human beta-galactosidase in complex with 1-2 deoxygalactonojirimycin	c3thdD crystal structure of human beta-galactosidase in complex with 1-2 deoxygalactonojirimycin	3thcA Crystal structure of human beta-galactosidase in complex with galactose	3thcA Crystal structure of human beta-galactosidase in complex with galactose
Confidence/Z-score	100%	100%	2.87	2.71	100.0%	100.0%	3.20	5.95
Coverage	86% (480 residues)	87% (462 residues)	0.87	0.87	89% (602 residues)	89% (602 residues)	0.89	0.89
Domain analysis identity	99%	99%	1.00	1.00	100%	99%	0.99	1.00
Secondary structure/ CS	Alpha helix/9	No/9	Helix/	Coil/9	Alpha helix/4	Alpha helix/7	Strand /7	Strand/3
Disordered prediction/CS	No/1	Disordered/9	–	–	None/1	None/1	–	–
Solvent accessibility score	–	–	4	5	–	–	0	0
Normalized B factor	—	–	−0.47	1.47			−0.54	−0.54
Functional analysis								
3DLigandSite/CS		1nouA/100.0	–	–			–	–
COACH (I-TASSER) ligand bindingPDB hit/C-score	–	–	3ozpA/0.62	1np0A/0.89	–	–	3thcA/0.86	3wezA/0.82
Enzyme commission PDB hit/ C-score^{EC}	–	–	1o7aA/0.651	1o7aA/0.617	–	–	1yq2A/0.379	1yq2A/0.380
Enzyme ontology PDBhit/C-score^{GO}	–	–	1o7aA/0.62	1o7aA/0.51	–	–	3d3aA/0.63	3d3aA/0.62

PDB: Protein Data Bank; CS: Confidence score.
Solvent accessibility: Values range from 0(buried residue) to 9 (highly exposed residue).
BFP: normalized B-Factor indicating residues with BFP values higher than 0 are less stable in experimental structures.
Threading Template: A template is made based on folds similarity of small segments of proteins.
Z-score: Alignment with a Normalized Z-score > 1 mean a good alignment and vice versa.
C-score: is the confidence score of the prediction. C-score ranges [0–1], where a higher score indicates a more reliable prediction.

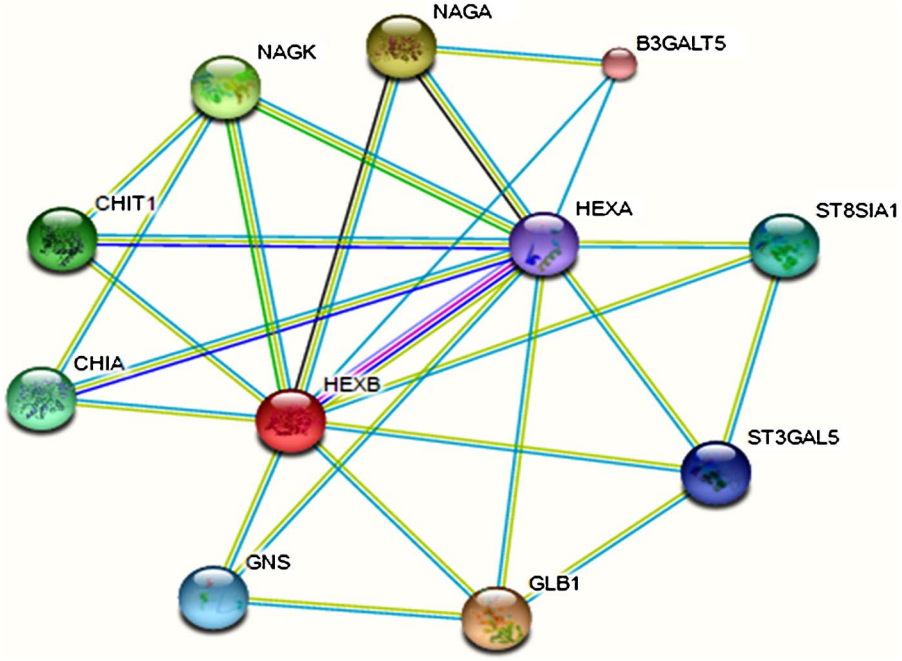

Fig. 3. The scheme of protein-protein interaction network of HEXB by STRING 10.0. Hexaminidase A (composed of alpha and beta chain) is lysosomal enzyme and affects neuronal cells. GLB1: galactosidase, beta 1- Cleaves beta-linked terminal galactosyl residues from gangliosides, glycoproteins, and glycosaminoglycans (677 aa); NAGA: *N*-acetylgalactosaminidase, alpha- Removes terminal alpha- *N*-acetylgalactosamine residues from glycolipids and glycopeptides. Required for the breakdown of glycolipids (411 aa); NAGK *N*-acetylglucosamine kinase-Converts endogenous *N*-acetylglucosamine (GlcNAc), a major component of complex carbohydrates, from lysosomal degradation or nutritional sources into GlcNAc 6-phosphate. Involved in the *N*-glycolylneuraminic acid (Neu5Gc) degradation pathway- although human is not able to catalyze formation of Neu5Gc due to the inactive CMAHP enzyme, Neu5Gc is present in food and must be degraded. Also has ManNAc kinase activity (390 aa); CHIT1: chitinase 1 (chitotriosidase) (466 aa); CHIA: chitinase, acidic (476 aa); ST8SIA1: ST8 alpha- *N*-acetyl-neuraminide alpha-2,8-sialyltransferase 1; Involved in the production of gangliosides GD3 and GT3 from GM3; gangliosides are a subfamily of complex glycosphinglolipds that contain one or more residues of sialic acid (356 aa); GNS:glucosamine (*N*-acetyl)-6-sulfatase (552 aa); ST3GAL5: ST3 beta-galactoside alpha-2,3-sialyltransferase 5; Catalyzes the formation of ganglioside GM3 (alpha- *N*-acetylneuraminyl-2,3-beta-D-galactosyl-1, 4-beta-D- glucosylceramide) (418 aa); HEXA hexosaminidase A (alpha polypeptide); Responsible for the degradation of GM2 gangliosides, and a variety of other molecules containing terminal *N*-acetyl hexosamines, in the brain and other tissues. The form B is active against certain oligosaccharides. The form S has no measurable activity (529 aa); B3GALT5: UDP-Gal-betaGlcNAc beta 1,3-galactosyltransferase, polypeptide 5; Catalyzes the transfer of Gal to GlcNAc-based acceptors with a preference for the core3 O-linked glycan GlcNAc(beta1,3) GalNAc structure. Can use glycolipid LC3Cer as an efficient acceptor (310 aa).

Ganglioside degradation occurs when GM2 activator protein (by its docking site) binds to GM2 gangliosides through terminal N-acetyl hexosaminidase residues. The activator interacts with both carbohydrate and lipid portion of ganglioside; then it interacts with the middle section of α-subunit and carboxyl half of the β-subunit of Hexosaminidase A [6]. In the quaternary structure of enzyme, docking reaction of activator is through between 280–400 residues on discrete patches on the α-subunit and through 465-545 residues of β-subunit [6]. The Beta subunit increases the affinity and orientation of the complex for the hydrolysis reaction [2,54,68]. This demonstrates that the beta subunit acts in structure of the complex but not the function directly; although any variant consequently would affect the function of beta. This updated analysis of *HEXB* variants shows that 25 mutations (23.36%) have been identified in the predicted docking site of HexB which can affect the efficient binding of activator to Hex A, and suggests that the β-subunit plays an important role in this process (Fig. 1).

Considering Cys534 of hexosaminidase β chain forms a disulfide bond to Cys551 which connects the C-terminal loop to core domain (central (β,α)8-barrel domain) of protein [27,68]. p.Cys534Ter could affect all the downstream residues from Cys551 to C terminus (residue 556) [6]. As noticed previously, amino acids from cys534 to C-termini (556) contribute in dimerization of two subunits (αβ in Hex A and ββ in Hex B). Dimerization is important for making a docking site for the activator. We postulate that this mutation may interrupt the dimerization and activator function, which consequently may lead to deficiency in both Hex A and Hex B enzymes. Cys534 is located in exon 13; this exon accounts for about 15.92% of the variants (Fig. 1). It contributes in HexB docking site which is among the frequent exons affecting the protein function. The other variant at position 284, also located in the a central $(\beta,\alpha)_8$-barrel domain which led to a stop codon influences all the central domain. As predicted by CADD, the PHRED score was 39 which shows that it is more deleterious.

Diagnosis of gangliosidosis is based on clinical features and biochemical and enzymatic profiles. The biochemical analysis for Case 1 showed the deficiency of HexA, and HexB clinically suspected of having B-gangliosidosis, though B-galactosidase deficiency was inconclusive since the enzyme assay was repeated twice. This made the diagnosis difficult; therefore, molecular genetic testing would help to establish the diagnosis.

In general, it is unclear that the gangliosidoses is caused by loss of enzyme activity, regulation of neuronal function, elevation of precursors or by an imbalance of glycosphingolipids ratio [69]. Clinical heterogeneity may be due to a variety of substrate specificities and functions of hydrolases, regulatory effects of associated proteins, and other lipids despite the genetic background [1]. Patterns of substrate accumulation somehow correlate to the pathological and biochemical phenotypes. To explain the B-galactosidose deficiency in Case 1. The substrate accumulated assessment in late GM1-gangliosidosis is relevant to biochemical phenotype correlation rather than the enzyme functions though this is vise versa for other substrates [1]. For example, in B-gangliosidose deficiency, GM1-ganglioside is sufficient but there is dysfunction of breakdown of other substrates which is not gangliosidosis but mucopolysaccharidosis IV type B [70,31,30,27] and/or sialidase deficiency which was noticed in other studies [71,32,31,28]. We conclude that the B-gangliosidase could be deficient in the patient although the variation was found in the *HEXB* gene.

Interactome analysis by STRING10 describes a network of functional proteins associated with *HEXB* including *GLB1* gene (galactosidase B1), *NAGA* (*N*-acetylgalactosaminidase alpha), *HEXA* (Hexaminidase *A*-alpha), *GNS* (glucosamine (*N*-acetyl)-6-sulfatase), *NAGK* (*N*-acetylglucosamine kinase), *CHIT1* (chitotriosidase), CHIA (chitinase, acidic), ST8SIA1 ST8 alpha-*N*-acetyl-neuraminide alpha-2,8-sialyltransferase 1; ST3GAL5 ST3 beta-galactoside alpha-2,3-sialyltransferase 5; B3GALT5 UDP-Gal-betaGlcNAc beta 1,3-galactosyltransferase, polypeptide 5 (Fig. 3). Enzymes and proteins involved in gangliosidosis may act in other pathways, therefore showing spectrum of phenotype. A complete description of clinical features and more evaluations are needed to draw a conclusion for genotype-phenotype correlations. As in the presented case, the clinical diagnosis was difficult due to inconsistency in enzyme assay.

Due to consanguineous marriages in Iranian population there may be a high incidence of lysosomal diseases. Other investigations show that GM2-Gangliosidoses is frequent in this population [24,72]. In another survey 18 patients from 2009 to 2014 referred due to GM2 gangliosidoses. Our referral center in Iran has had 37 gangliosidosis patients from 2011 to 2016 (unpublished data). Therefore, a screening

program would increase the health status in this region of the world and reduce the psychological and economical influences in the affected families and society. Tandem mass spectrometry (MS/MS) is being used for newborn screening of treatable pediatric disorders in presymptomatic newborns. A rapid technology for the analysis of amino acid and acylcarnitine profiles for identification of 40 different inborn errors of amino acid, fatty acid, and organic acid metabolism [73,74]. Treatable conditions have progressed for previously untreatable disorders which lead to newborn screening of several conditions with a strong neuronopathic, lysosomal storage and metabolic disorders [75,76]. Usually newborn screening programs are included for the frequent disorders in the country, meant to detect inborn disorders that can result in early mortality or lifelong disability. Enzyme replacement, substrate reducing therapy, pharmacological chaperons, bone marrow transplantation, and anti-inflammatory drugs are strategies for therapy of gangliosidosis and lysosomal storage disorders; although there are obstacles to therapy [48].

Molecular based testing can be used to confirm the clinical diagnosis of clinically heterogeneous disorders. In uncertain cases, genetic testing with panel based next generation sequencing can establish a diagnosis, especially in milder or atypical phenotypes. Molecular genetic testing gives insights into confirmation of diagnosis for better management of patients, carrier detection, and family planning and plays a fundamental role in prenatal diagnosis. Molecular genetic testing of *HEXA* and *HEXB* is primarily to distinguish psuedodeficiency alleles from causal variants in affected and unaffected individuals to allow genetic counseling of at risk families and family members.

Acknowledgments

We appreciate Dr. Cynthia J. Tifft and Dr. Christina Grant (National Human Genome Research Institute) for critical comments and reading the manuscript. We also thank laboratory staffs in Rajaie Hospital.

References

[1] K. Sandhoff, K. Harzer, Gangliosides and gangliosidoses: principles of molecular and metabolic pathogenesis, J. Neurosci. 33 (2013) 10195–10208.
[2] D.J. Mahuran, Biochemical consequences of mutations causing the GM2 gangliosidoses, Biochim. Biophys Acta 1455 (1999) 105–138.
[3] H.H. Heng, B. Xie, X.M. Shi, L.C. Tsui, D.J. Mahuran, Refined mapping of the GM2 activator protein (GM2A) locus to 5q31.3-q33.1, distal to the spinal muscular atrophy locus, Genomics 18 (1993) 429–431.
[4] C. Scriver, A. Beaudet, W. Sly, The Metabolic and Molecular Bases of Inherited Disease, 7th ed., McGraw Hill, New York, 1995.
[5] R.L. Proia, Gene encoding the human beta-hexosaminidase beta chain: extensive homology of intron placement in the alpha- and beta-chain genes, Proc. Natl. Acad. Sci. U. S. A. 85 (1988) 1883–1887.
[6] B.L. Mark, D.J. Mahuran, M.M. Cherney, D. Zhao, S. Knapp, M.N. James, Crystal structure of human beta-hexosaminidase B: understanding the molecular basis of Sandhoff and Tay-Sachs disease, J. Mol. Biol. 327 (2003) 1093–1109.
[7] R.G. Korneluk, D.J. Mahuran, K. Neote, M.H. Klavins, B.F. O'Dowd, M. Tropak, H.F. Willard, M.J. Anderson, J.A. Lowden, R.A. Gravel, Isolation of cDNA clones coding for the alpha-subunit of human beta-hexosaminidase. Extensive homology between the alpha- and beta-subunits and studies on Tay-Sachs disease, J. Biol. Chem. 261 (1986) 8407–8413.
[8] J.Q. Huang, J.M. Trasler, S. Igdoura, J. Michaud, N. Hanal, R.A. Gravel, Apoptotic cell death in mouse models of GM2 gangliosidosis and observations on human Tay-Sachs and Sandhoff diseases, Hum. Mol. Genet. 6 (1997) 1879–1885.
[9] H. Li, R. Durbin, Fast and accurate short read alignment with burrows-wheeler transform, Bioinformatics 25 (2009) 1754–1760.
[10] H. Li, B. Handsaker, A. Wysoker, T. Fennell, J. Ruan, N. Homer, G. Marth, G. Abecasis, R. Durbin, S. Genome Project Data Processing, The sequence alignment/map format and SAMtools, Bioinformatics 25 (2009) 2078–2079.
[11] P. Gupta, P.S.N. Menon, S. Ramji, PG Textbook of Pediatrics, 1 ed., Jaypee Brothers Medical Pub, 2015.
[12] C. Genomes Project, A. Auton, L.D. Brooks, R.M. Durbin, E.P. Garrison, H.M. Kang, J.O. Korbel, J.L. Marchini, S. McCarthy, G.A. McVean, G.R. Abecasis, A global reference for human genetic variation, Nature 526 (2015) 68–74.
[13] J.M. Schwarz, D.N. Cooper, M. Schuelke, D. Seelow, MutationTaster2: mutation prediction for the deep-sequencing age, Nat. Methods 11 (2014) 361–362.
[14] N.L. Sim, P. Kumar, J. Hu, S. Henikoff, G. Schneider, P.C. Ng, SIFT web server: predicting effects of amino acid substitutions on proteins, Nucleic Acids Res. 40 (2012) W452–W457.
[15] Y. Choi, G.E. Sims, S. Murphy, J.R. Miller, A.P. Chan, Predicting the functional effect of amino acid substitutions and indels, PLoS One 7 (2012) e46688.
[16] M. Kircher, D.M. Witten, P. Jain, B.J. O'Roak, G.M. Cooper, J. Shendure, A general framework for estimating the relative pathogenicity of human genetic variants, Nat. Genet. 46 (2014) 310–315.
[17] L.A. Kelley, M.J. Sternberg, Protein structure prediction on the Web: a case study using the Phyre server, Nat. Protoc. 4 (2009) 363–371.
[18] L.A. Kelley, S. Mezulis, C.M. Yates, M.N. Wass, M.J. Sternberg, The Phyre2 web portal for protein modeling, prediction and analysis, Nat. Protoc. 10 (2015) 845–858.
[19] A. Roy, A. Kucukural, Y. Zhang, I-TASSER: a unified platform for automated protein structure and function prediction, Nat. Protoc. 5 (2010) 725–738.
[20] D. Szklarczyk, A. Franceschini, S. Wyder, K. Forslund, D. Heller, J. Huerta-Cepas, M. Simonovic, A. Roth, A. Santos, K.P. Tsafou, M. Kuhn, P. Bork, L.J. Jensen, C. von Mering, STRING v10: protein-protein interaction networks, integrated over the tree of life, Nucleic Acids Res. 43 (2015) D447–D452.
[21] B.B. Fitterer, N.A. Antonishyn, P.L. Hall, D.C. Lehotay, A polymerase chain reaction-based genotyping assay for detecting a novel Sandhoff disease-causing mutation, Genet. Test Mol. Biomarkers 16 (2012) 401–405.
[22] L. Gort, N. de Olano, J. Macias-Vidal, M.A. Coll, G.M.W.G. Spanish, GM2 gangliosidoses in Spain: analysis of the HEXA and HEXB genes in 34 Tay-Sachs and 14 Sandhoff patients, Gene 506 (2012) 25–30.
[23] P. Gaignard, J. Fagart, N. Niemir, J.P. Puech, E. Azouguene, J. Dussau, C. Caillaud, Characterization of seven novel mutations on the HEXB gene in French Sandhoff patients, Gene 512 (2013) 521–526.
[24] H. Aryan, O. Aryani, K. Banihashemi, T. Zaman, M. Houshmand, Novel mutations in Sandhoff disease: a molecular analysis among Iranian cohort of infantile patients, Iran J. Public Health 41 (2012) 112–118.
[25] C.R. Scriver, The Metabolic & Molecular Bases of Inherited Disease, Montreal: McGraw-Hill, New York, 2001.
[26] A.K. Sobek, C. Evers, G. Dekomien, Integrated multiplex ligation dependent probe amplification (MLPA) assays for the detection of alterations in the HEXB, GM2A and SMARCAL1 genes to support the diagnosis of Morbus Sandhoff, M. Tay-Sachs variant AB and Schimke immuno-osseous dysplasia in humans, Mol. Cell. Probes 27 (2013) 32–37.
[27] S. Zampieri, S. Cattarossi, A.M. Oller Ramirez, C. Rosano, C.M. Lourenco, N. Passon, I. Moroni, G. Uziel, A. Pettinari, F. Stanzial, R.D. de Kremer, N.B. Azar, F. Hazan, M. Filocamo, B. Bembi, A. Dardis, Sequence and copy number analyses of HEXB gene in patients affected by Sandhoff disease: functional characterization of 9 novel sequence variants, PLoS One 7 (2012) e41516.
[28] Y. Huang, T. Xie, J. Zheng, X. Zhao, H. Liu, L. Liu, Clinical and molecular characteristics of a child with juvenile Sandhoff disease, Zhonghua Er Ke Za Zhi 52 (2014) 313–316.
[29] Y. Hara, P. Ioannou, A. Drousiotou, G. Stylianidou, V. Anastasiadou, K. Suzuki, Mutation analysis of a Sandhoff disease patient in the Maronite community in Cyprus, Hum. Genet. 94 (1994) 136–140.
[30] M. Gomez-Lira, M. Mottes, C. Perusi, P.F. Pignatti, N. Rizzuto, R. Gatti, A. Salviati, A novel 4-bp deletion creates a premature stop codon and dramatically decreases HEXB mRNA levels in a severe case of Sandhoff disease, Mol. Cell. Probes 15 (2001) 75–79.
[31] B. McInnes, C.A. Brown, D.J. Mahuran, Two small deletion mutations of the HEXB gene are present in DNA from a patient with infantile Sandhoff disease, Biochim. Biophys. Acta 1138 (1992) 315–317.
[32] C.A. Brown, B. McInnes, R.D. de Kremer, D.J. Mahuran, Characterization of two HEXB gene mutations in Argentinean patients with Sandhoff disease, Biochim. Biophys. Acta 1180 (1992) 91–98.
[33] C.J. Bell, D.L. Dinwiddie, N.A. Miller, S.L. Hateley, E.E. Ganusova, J. Mudge, R.J. Langley, L. Zhang, C.C. Lee, F.D. Schilkey, V. Sheth, J.E. Woodward, H.E. Peckham, G.P. Schroth, R.W. Kim, S.F. Kingsmore, Carrier testing for severe childhood recessive diseases by next-generation sequencing, Sci. Transl. Med. 3 (2011) 65ra64.
[34] S. Zampieri, M. Filocamo, E. Buratti, M. Stroppiano, K. Vlahovicek, N. Rosso, E. Bignulin, S. Regis, F. Carnevale, B. Bembi, A. Dardis, Molecular and functional analysis of the HEXB gene in Italian patients affected with Sandhoff disease: identification of six novel alleles, Neurogenetics 10 (2009) 49–58.
[35] N. Kaya, M. Al-Owain, N. Abudheim, J. Al-Zahrani, D. Colak, M. Al-Sayed, A. Milanlioglu, P.T. Ozand, F.S. Alkuraya, GM2 gangliosidosis in Saudi Arabia: multiple mutations and considerations for future carrier screening, Am. J. Med. Genet. A 155A (2011) 1281–1284.
[36] Z.X. Zhang, N. Wakamatsu, E.H. Mules, G.H. Thomas, R.A. Gravel, Impact of premature stop codons on mRNA levels in infantile Sandhoff disease, Hum. Mol. Genet. 3 (1994) 139–145.
[37] P.M. Tamhankar, M. Mistri, P. Kondurkar, D. Sanghavi, J. Sheth, Clinical, biochemical and mutation profile in Indian patients with Sandhoff disease, J. Hum. Genet. 61 (2016) 163–166.
[38] A. Ankala, J.N. Kohn, A. Hegde, A. Meka, C.L. Ephrem, S.H. Askree, S. Bhide, M.R. Hegde, Aberrant firing of replication origins potentially explains intragenic nonrecurrent rearrangements within genes, including the human DMD gene, Genome Res. 22 (2012) 25–34.
[39] E.H. Lee, J.H. Park, C.J. Coe, S.H. Hahn, A novel mutation in the beta-hexosaminidase beta-subunit gene in a 14-month-old Korean boy with Sandhoff disease: first reported Korean case, Hum. Mutat. 16 (2000) 180–181.
[40] K. Neote, B. McInnes, D.J. Mahuran, R.A. Gravel, Structure and distribution of an Alu-type deletion mutation in Sandhoff disease, J. Clin. Invest. 86 (1990) 1524–1531.
[41] Z.X. Zhang, N. Wakamatsu, B.R. Akerman, E.H. Mules, G.H. Thomas, R.A. Gravel, A second, large deletion in the HEXB gene in a patient with infantile Sandhoff disease,

Hum. Mol. Genet. 4 (1995) 777–780.
[42] H. Bikker, F.M. van den Berg, R.A. Wolterman, J.J. de Vijlder, P.A. Bolhuis, Demonstration of a Sandhoff disease-associated autosomal 50-kb deletion by field inversion gel electrophoresis, Hum. Genet 81 (1989) 287–288.
[43] B. Dlott, A. d'Azzo, D.V. Quon, E.F. Neufeld, Two mutations produce intron insertion in mRNA and elongated beta-subunit of human beta-hexosaminidase, J. Biol. Chem. 265 (1990) 17921–17927.
[44] M. Fujimaru, A. Tanaka, K. Choeh, N. Wakamatsu, H. Sakuraba, G. Isshiki, Two mutations remote from an exon/intron junction in the beta-hexosaminidase beta-subunit gene affect 3'-splice site selection and cause Sandhoff disease, Hum. Genet. 103 (1998) 462–469.
[45] G.H. Maegawa, M. Tropak, J. Buttner, T. Stockley, F. Kok, J.T. Clarke, D.J. Mahuran, Pyrimethamine as a potential pharmacological chaperone for late-onset forms of GM2 gangliosidosis, J. Biol. Chem. 282 (2007) 9150–9161.
[46] P. Banerjee, L. Siciliano, D. Oliveri, N.R. McCabe, M.J. Boyers, A.L. Horwitz, S.C. Li, G. Dawson, Molecular basis of an adult form of beta-hexosaminidase B deficiency with motor neuron disease, Biochem. Biophys. Res. Commun. 181 (1991) 108–115.
[47] W. Zhang, H. Zeng, Y. Huang, T. Xie, J. Zheng, X. Zhao, H. Sheng, H. Liu, L. Liu, Clinical, biochemical and molecular analysis of five Chinese patients with Sandhoff disease, Metab. Brain Dis. 31 (4) (2016) 861–867.
[48] R.M. Boustany, Lysosomal storage diseases–the horizon expands, Nat. Rev. Neurol. 9 (2013) 583–598.
[49] S.B. Wortmann, D.J. Lefeber, G. Dekomien, M.A. Willemsen, R.A. Wevers, E. Morava, Substrate deprivation therapy in juvenile Sandhoff disease, J. Inherit. Metab. Dis. 32 (Suppl. 1) (2009) S307–S311.
[50] M. Gomez-Lira, A. Sangalli, M. Mottes, C. Perusi, P.F. Pignatti, N. Rizzuto, A. Salviati, A common beta hexosaminidase gene mutation in adult Sandhoff disease patients, Hum. Genet. 96 (1995) 417–422.
[51] S.Z. Wang, M.B. Cachon-Gonzalez, P.E. Stein, R.H. Lachmann, P.C. Corry, J.E. Wraith, T.M. Cox, A novel HEXB mutation and its structural effects in juvenile Sandhoff disease, Mol. Genet. Metab. 95 (2008) 236–238.
[52] M. Beker-Acay, M. Elmas, R. Koken, E. Unlu, A. Bukulmez, Infantile type Sandhoff disease with striking brain MRI findings and a novel mutation, Pol. J. Radiol. 81 (2016) 86–89.
[53] M. Santoro, A. Modoni, M. Sabatelli, F. Madia, F. Piemonte, G. Tozzi, E. Ricci, P.A. Tonali, G. Silvestri, Chronic GM2 gangliosidosis type Sandhoff associated with a novel missense HEXB gene mutation causing a double pathogenic effect, Mol. Genet. Metab. 91 (2007) 111–114.
[54] Y. Hou, B. McInnes, A. Hinek, G. Karpati, D. Mahuran, A Pro504 –& Ser substitution in the beta-subunit of beta-hexosaminidase A inhibits alpha-subunit hydrolysis of GM2 ganglioside, resulting in chronic Sandhoff disease, J. Biol. Chem. 273 (1998) 21386–21392.
[55] P.A. Bolhuis, N.J. Ponne, H. Bikker, F. Baas, J.M. Vianney de Jong, Molecular basis of an adult form of Sandhoff disease: substitution of glutamine for arginine at position 505 of the beta-chain of beta-hexosaminidase results in a labile enzyme, Biochim. Biophys. Acta 1182 (1993) 142–146.
[56] T. Yoshizawa, Y. Kohno, S. Nissato, S. Shoji, Compound heterozygosity with two novel mutations in the HEXB gene produces adult Sandhoff disease presenting as a motor neuron disease phenotype, J. Neurol. Sci. 195 (2002) 129–138.
[57] Y. Kuroki, K. Itoh, Y. Nadaoka, T. Tanaka, H. Sakuraba, A novel missense mutation (C522Y) is present in the beta-hexosaminidase beta-subunit gene of a Japanese patient with infantile Sandhoff disease, Biochem. Biophys. Res. Commun. 212 (1995) 564–571.
[58] B. Fitterer, P. Hall, N. Antonishyn, R. Desikan, M. Gelb, D. Lehotay, Incidence and carrier frequency of Sandhoff disease in Saskatchewan determined using a novel substrate with detection by tandem mass spectrometry and molecular genetic analysis, Mol. Genet. Metab. 111 (2014) 382–389.
[59] G. Narkis, A. Adam, L. Jaber, M. Pennybacker, R.L. Proia, R. Navon, Molecular basis of heat labile hexosaminidase B among Jews and Arabs, Hum. Mutat. 10 (1997) 424–429.
[60] T. Wu, X. Li, Q. Wang, Y. Liu, Y. Ding, J. Song, Y. Zhang, Y. Yang, HEXB gene study and prenatal diagnosis for a family affected by infantile Sandhoff disease, Zhejiang Da Xue Xue Bao Yi Xue Ban 42 (2013) 403–410.
[61] H.F. Lee, C.S. Chi, C.R. Tsai, Early cardiac involvement in an infantile Sandhoff disease case with novel mutations, Brain Dev. (2016).
[62] F.E. Kleiman, R.D. de Kremer, A.O. de Ramirez, R.A. Gravel, C.E. Argarana, Sandhoff disease in Argentina: high frequency of a splice site mutation in the HEXB gene and correlation between enzyme and DNA-based tests for heterozygote detection, Hum. Genet. 94 (1994) 279–282.
[63] K. Furihata, A. Drousiotou, Y. Hara, G. Christopoulos, G. Stylianidou, V. Anastasiadou, I. Ueno, P. Ioannou, Novel splice site mutation at IVS8 nt 5 of HEXB responsible for a Greek-Cypriot case of Sandhoff disease, Hum. Mutat. 13 (1999) 38–43.
[64] M. Gomez-Lira, C. Perusi, M. Mottes, P.F. Pignatti, N. Rizzuto, R. Gatti, A. Salviati, Splicing mutation causes infantile Sandhoff disease, Am. J. Med. Genet 75 (1998) 330–333.
[65] N. Wakamatsu, H. Kobayashi, T. Miyatake, S. Tsuji, A novel exon mutation in the human beta-hexosaminidase beta subunit gene affects 3' splice site selection, J. Biol. Chem. 267 (1992) 2406–2413.
[66] T. Nakano, K. Suzuki, Genetic cause of a juvenile form of Sandhoff disease. Abnormal splicing of beta-hexosaminidase beta chain gene transcript due to a point mutation within intron 12, J. Biol Chem. 264 (1989) 5155–5158.
[67] M. Gomez-Lira, C. Perusi, N. Brutti, M.A. Farnetani, M.A. Margollicci, N. Rizzuto, P.F. Pignatti, A. Salviati, A 48-bp insertion between exon 13 and 14 of the HEXB gene causes infantile-onset Sandhoff disease, Hum. Mutat. 6 (1995) 260–262.
[68] T. Maier, N. Strater, C.G. Schuette, R. Klingenstein, K. Sandhoff, W. Saenger, The X-ray crystal structure of human beta-hexosaminidase B provides new insights into Sandhoff disease, J. Mol. Biol. 328 (2003) 669–681.
[69] R.L. Proia, Gangliosides help stabilize the brain, Nat. Genet. 36 (2004) 1147–1148.
[70] Y. Suzuki, A. Oshima, E. Nanba, Beta-galactosidase deficiency (beta-galactosidosis): GM1 gangliosidosis and Morquio B disease, in: C. Scriver, A. Beaudet, W. Sly, D. Valle (Eds.), The Metabolic and Molecular Bases of Inherited Disease, McGraw-Hill, New York, 2001, pp. 3775–3809.
[71] A. d'Azzo, G. Andria, P. Strisciuglio, H. Galjaard, Galactosialidosis, in: C. Scriver, A. Beaudet, W. Sly, D. Valle (Eds.), The Metabolic & Molecular Bases of Inherited Disease, McGraw-Hill, New York, 2001, p. 3811.
[72] P. Karimzadeh, N. Jafari, H. Biglari-Nejad, S. Jabbehdari, F. Ahmad abadi, M.-R. Alaee, H. Nemati, S. Saket, S.H. Tonekaboni, M.-M. Taghdiri, GM2-gangliosidosis (Sandhoff and Tay Sachs disease): diagnosis and neuroimaging findings (an Iranian pediatric case series), Iran. J. Child Neurol. 8 (2014) 55–60.
[73] D.H. Chace, T.A. Kalas, E.W. Naylor, The application of tandem mass spectrometry to neonatal screening for inherited disorders of intermediary metabolism, Annu. Rev. Genomics Hum. Genet. 3 (2002) 17–45.
[74] C. Turgeon, M.J. Magera, P. Allard, S. Tortorelli, D. Gavrilov, D. Oglesbee, K. Raymond, P. Rinaldo, D. Matern, Combined newborn screening for succinylacetone, amino acids, and acylcarnitines in dried blood spots, Clin. Chem. 54 (2008) 657–664.
[75] M.H. Gelb, C.R. Scott, F. Turecek, Newborn screening for lysosomal storage diseases, Clin. Chem. 61 (2015) 335–346.
[76] D. Matern, D. Oglesbee, S. Tortorelli, Newborn screening for lysosomal storage disorders and other neuronopathic conditions, Dev. Disabil. Res. Rev. 17 (2013) 247–253.